Hindawi Publishing Corporation
Journal of Nanomaterials
Volume 2015, Article ID 963012, 6 pages
http://dx.doi.org/10.1155/2015/963012

Research Article

A Novel Porous Carrier Found in Nature for Nanocomposite Materials Preparation: A Case Study of *Artemia* Egg Shell-Supported TiO_2 for Formaldehyde Removal

Sufeng Wang, Fengjing Lv, Tifeng Jiao, Jingfen Ao, Xiaochun Zhang, and Fengdan Jin

Hebei Key Laboratory of Applied Chemistry, School of Environmental and Chemical Engineering, Yanshan University, Qinhuangdao 066004, China

Correspondence should be addressed to Sufeng Wang; sfwang@ysu.edu.cn

Received 17 July 2014; Revised 20 August 2014; Accepted 20 August 2014

Academic Editor: Xinqing Chen

Artemia egg shells have an asymptotic sized pore structure (pore diameter: 500 nm–2500 nm), which could be used as a porous carrier for the preparation of nanocomposite materials. The objective of the present study was to prepare shell-supported TiO_2 using a naturally porous carrier, *Artemia* egg shell, and to exhibit a case study of shell-supported TiO_2 for formaldehyde removal. Characterization of shell-TiO_2 using SEM-EDS, TEM, and XRD proved that *Artemia* shell with asymptotic reduction pores (pore diameter: 500 nm–2500 nm) can be used as the carrier for nanocomposite materials. *Artemia* egg shell-supported TiO_2 in polycrystalline-like nanostructures can be used for the high efficiency removal (adsorption and degradation) of formaldehyde under visible light. Our results suggest that iron, one of the shell's components, should broaden the absorption of visible light and enhance the photocatalytic efficiency of nanotitanium dioxide under visible light. Due to their interesting absorption and formaldehyde removal qualities, *Artemia* egg shell, as a novel naturally porous carrier for nanocomposite materials preparation, especially in the preparation of nanocatalysts, is worthy of further study.

1. Introduction

The rapidly advancing field of nanotechnology has great promise for environmental remediation [1–6]. Supporter-immobilized inorganic adsorbents are one of the main environmental applications of nanotechnologies that attempt to solve the existing problems of neat nanoparticles [2, 4, 7] such as poor mechanical strength, pore collapsing, particle crush, and particles flowing away. In previous studies, researchers have loaded zirconium, iron, and cadmium onto the porous surfaces of collagen fibers, zeolite, polymer, ceramics, activated carbon, and other porous materials as a functional composite adsorbent and examined the adsorbent function for the removal of pollution [1–6]. In these studies, it was proved that the adsorptive function of composite adsorbent-based carriers is more efficient than nano-inorganic adsorbents alone [4–7]. Moreover, different carrier-supported materials showed different material-dependent performances [2]. These issues of differing performances mean that the carrier selected to support inorganic adsorbents became the main problem.

Artemia, member of the crustacean subphylum, mainly live in coastal waters, salt ponds, and plateau salt lakes. *Artemia* are globally plentiful and it has been recorded that their habitats encompass about 600 localities around the world [8, 9]. The annual harvest yield from natural and aquacultural sources of living *Artemia* and *Artemia* eggs is about 15000 t and 300–500 t, respectively, in China alone. Unique multipore layers in *Artemia* egg shells have been reported [9–13], and researchers have documented that the pores of *Artemia* egg shells appeared to have an asymptotic size distribution (diameter: 500 nm–2500 nm) [9, 13]. In addition, *Artemia* egg shells have multiple outstanding capabilities such as nice biocompatibility, environmentally friendly characteristics, and excellent stability [14, 15]. However, when *Artemia* egg was hatched for aquacultural living food, *Artemia* egg shells have been disposed of as a waste. *Artemia* egg shells, with their novel naturally porous

structure, are worthy of further study as the carrier for nanocomposite materials in pollution removal applications.

Indoor air pollution presents an important domestic environmental concern [16, 17], since people are decorating their living spaces with plywood, coating materials, paint, and the other materials that may contain volatile organic compounds (VOCs), such as formaldehyde, benzene, and ketones. These VOCs being released from decorative materials pollute the indoor air and harm the health of inhabitants. This indicates a clear need for novel indoor air pollution remediation technologies.

One of the nano-inorganic adsorbents most commonly used in indoor harmful gas removal is nanoscale titanium dioxide (nano-TiO_2) because of its adsorption properties and degradation as a photo-catalytic [18]. Theoretically, nano-TiO_2 could provide more active surface sites for photodegradation through diffusion [19]. However, ultra-fine TiO_2 powders with large specific surface areas agglomerate easily, and its adverse effect on their catalytic performance has been observed [19, 20]. Therefore, carrier-supported TiO_2 could be used to avoid the defects stated above.

In the present paper, the composite materialswere fabricated by loading nano-TiO_2 onto the porous surface of *Artemia* egg shells and a case study of *Artemia* egg shell-supported TiO_2 for formaldehyde removal was actualized.

2. Materials and Methods

2.1. Materials. *Artemia* shells were collected from the Beidaihe Central Experiment Station of the Chinese Academy of Fishery Science. Before the experiments, shells were subjected to flushing with freshwater to remove the residual impurities (including salts). All treated shells were rewashed with deionized H_2O until they reached a constant neutral pH in the range of 6.8–7.2 and vacuum desiccated at 70°C for 24 hr until reaching a constant weight.

All chemicals are of analytical grade from Aladdin Reagent Station (Beijing, China), and the orthophosphate solution (1000 mg/L) was prepared by dissolving KH_2PO_4 into the deionized water.

2.2. Preparation of Shell-TiO_2 Composite Materials. For shell-TiO_2 composite materials fabrication, 0.2 g of egg shells was immersed in a mixture of blended 5 mL butyl titanate, 20 mL absolute ethyl alcohol, and 0.5 mL hydrochloric acid (37%). Hydrochloric acid was used to prevent the butyl titanate from hydrolyzing in the absolute ethyl alcohol before the titanate could get into the egg shells. The egg shell mixture was dispersed by ultrasound (40 KHz, 50 W, 50°C) for 2 hr. Then, the butyl titanate-sucking egg shells were screened and washed with absolute ethyl alcohol and put into a 5% NaOH solution with magnetic stirring. The NaOH solution was used to accelerate the hydrolysis of the butyl titanate-sucking egg shells. After being screened and washed by the deionized H_2O, egg shells with TiO_2 (the product of the hydrolysis) were desiccated at 80°C for 24 hr until reaching a constant weight. The calcination of shell-TiO_2 was carried out under an anoxic environment inside a Muffle Furnace at 500°C for 2 hr.

2.3. Characterization of Shell-TiO_2 Composite Materials. The morphology and property characterization of shell-TiO_2 composite materials were completed using a field emission scanning electron microscope (SEM) with an energy dispersive X-ray spectrometer (EDS). All SEM specimens were mounted on standard copper stubs, coated with a layer of gold/palladium about 5 nm think, and observed under SEM (S-4800 II, Hitachi, Japan). The chemical composition of the composite materials was characterized by EDS (Horiba, Japan), which was typically performed at an accelerating voltage of 20 kV, using an Oxford Link-ISIS X-ray EDXS microanalysis system attached to the SEM.

The TiO_2 particles loaded onto the porous surface of *Artemia* egg shells were observed with a transmission electron microscope (TEM). TEM images were recorded using a high-resolution transmission electron microscope (HRTEM, JEM2010) equipped with a Gatan CCD camera and working at an accelerating voltage of 20 kV.

The crystalline of TiO_2 particles loaded onto the porous surface of *Artemia* egg shells was characterized by X-ray diffraction (XRD) using an XTRA X-ray diffractometer (Rigaku Inc., Tokyo, Japan). The XRD pattern was obtained using Cu$K\alpha$ radiation with an incident wavelength of 0.1542 nm under a voltage of 40 kV and a current of 30 mA. The scan rate was 0.02°/min.

The control group for the above procedures was neat *Artemia* egg shells (no TiO_2) and was treated the same way as the shell-TiO_2 composites.

2.4. Formaldehyde Removal Experiments. The removal of formaldehyde using shell-TiO_2 composite materials was carried out in an illumination culture box (GXZ-280A, Ningbo Jiangnan Co., Zhejiang, China). 0.5 mL of 36% formaldehyde was dropped into a narrow-mouth bottle (10000 mL); after formaldehyde inpouring, the narrow-mouth bottle was sealed with a silicon stopper and parafilm. A uniform rubber tube was passed through the silicon stopper before formaldehyde inpouring, and the rubber tube was linked with a KC-6D air sampler (Laoshan Electron Instrument factory, Qingdao, China). A clamp was clamped to the rubber tube between the bottle mouth and the air sampler for sample control. The sealed narrow-mouth bottle was placed in darkness at 25°C for 5 days (until the formaldehyde volatilized evenly). For formaldehyde removal, 0.25 g of shell-TiO_2 composite material was spread evenly on a glass plate with double sided adhesive tape. Next, the glass plate with the shell-TiO_2 composite material coating was put into the formaldehyde-bottle, which was then airproofed again. Air samples (flow rate: 0.2 L/min and sample time: 1.5 min) were taken from each test bottle at intervals of 1 hr by the air sampler, and the removing rate was assayed by the phenol reagent spectrophotometric method.

Formaldehyde removal (%) was calculated by

$$\frac{C_t - C_0}{C_t} \times 100\%, \quad (1)$$

where C_0 is the initial of formaldehyde concentration in narrow-mouth bottle and C_t is the formaldehyde concentrations at the time of sample taken.

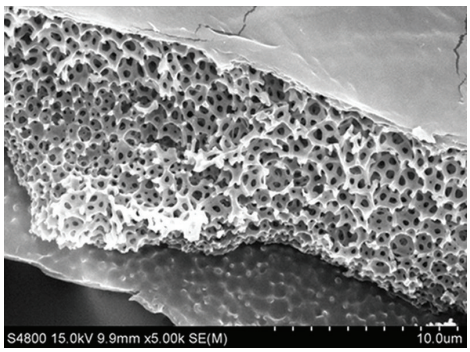

(a)

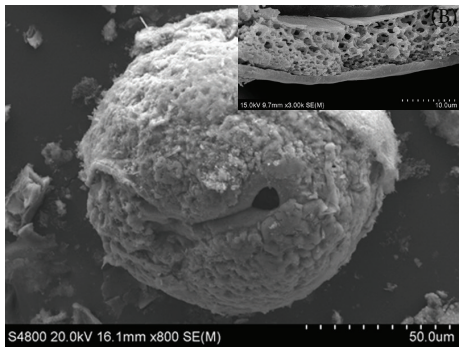

(b)

FIGURE 1: SEM images of (a) neat *Artemia* egg shell and (b) the shell-TiO_2 composite material.

The experiment was conducted in 2 replicates. One set of the formaldehyde removal experiments was carried out in darkness at 25°C; another set was actualized at 25°C under continuous illumination (about 1500 lx).

2.5. Data Analysis. Statistical analysis for formaldehyde removal was performed by SPSS 11.0 statistical software. Means were analyzed by descriptives and data are expressed as mean ± sem ($n = 3$).

3. Results and Discussion

3.1. Characterization of Shell-TiO_2 Composite Material. The shell-TiO_2 composite material prepared in the present study was characterized by SEM-EDS, TEM, and XRD analysis. As depicted in Figure 1(b)(B), the porous region within the shell-TiO_2 composite material was filled up with TiO_2 particles. Comparatively, the surface topography of the neat *Artemia* shell showed a smooth surface without any decorations (Figure 1(a)). This suggests that TiO_2 particles have considerably filled the pores of the *Artemia* egg shells.

Titanium element scanning of the cross section with SEM-EDS (Figures 2(a)–2(d)) further demonstrates that the TiO_2 particles were fabricated in the porous region of the *Artemia* shells. The spectrum of the shell-TiO_2 composite material shows the relative elemental abundance of titanium at high levels (Figures 2(c), and 2(d)), whereas the "site of interest 1" spectrum of neat *Artemia* shell (Figures 2(a), and

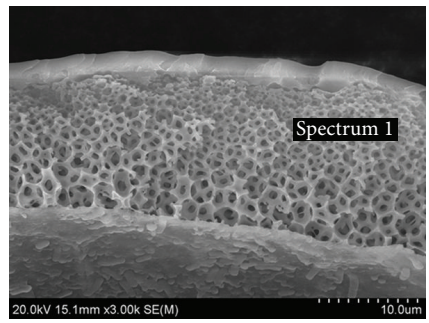

Electron image 1

(a)

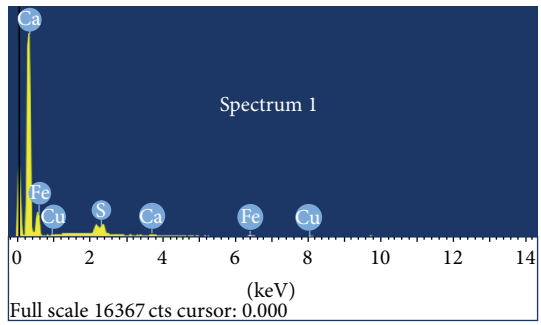

(b)

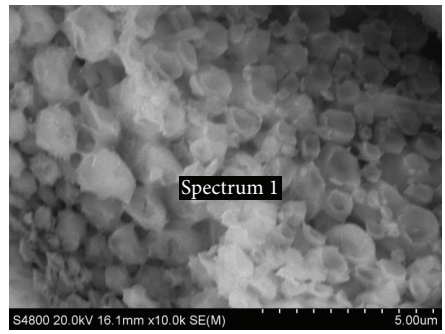

Electron image 1

(c)

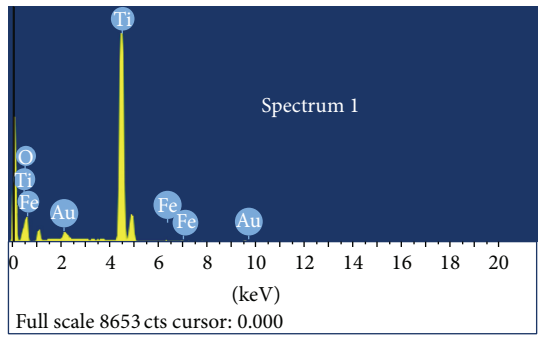

(d)

FIGURE 2: Representative SEM-EDS images and spectra highlighting titanium levels: SEM image of *Artemia* egg shell (a) and EDS element scanning of a cross section (b); SEM image of shell-TiO_2 composite material (c) and EDS element scanning of a cross section (d).

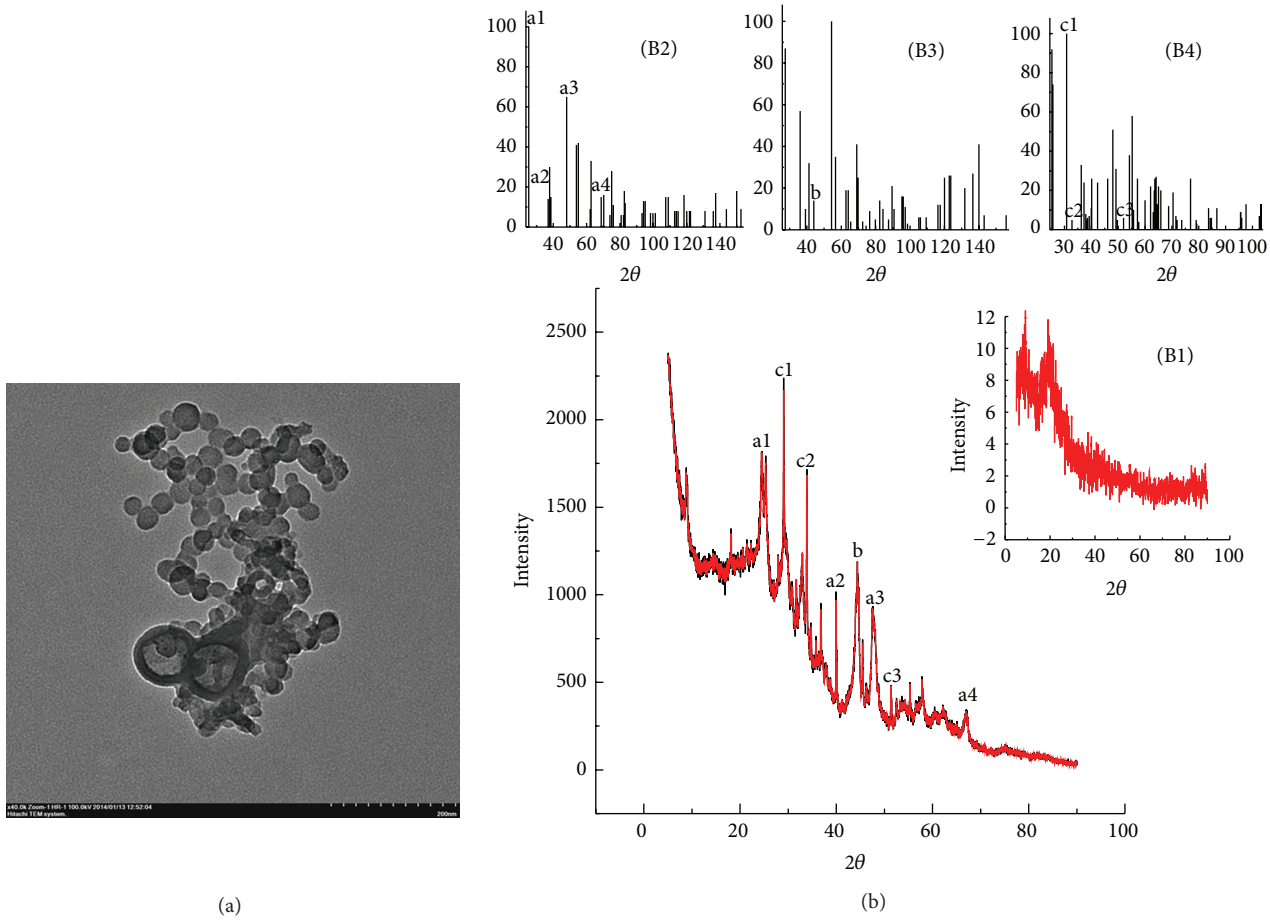

FIGURE 3: TEM images and XRD patterns of TiO_2 loaded onto the porous surface of *Artemia* egg shell: (a) TEM image of TiO_2 loaded onto the porous surface of *Artemia* egg shell; (b) XRD patterns of TiO_2 loaded onto the porous surface of *Artemia* egg shell; (B1) neat *Artemia* egg shell; (B2) standard card of anatase; (B3) standard card of rutile; and (B4) standard card of brookite.

2(b)) shows that there is no titanium in the shell pores. It appeared that the analysis of SEM-EDS corroborated the observations seen in the SEM images. The SEM image of shell-TiO_2 (Figure 2(c)) shows that the TiO_2 particles can be found everywhere within the shell pores especially when compared with the SEM image of neat *Artemia* shell (Figure 2(a)). The coverage of TiO_2 particles, spreading all over the porous region, implies that the diffusion of butyl titanate for TiO_2 formation into the deep area (the minimum pores layer) of the shell might not be restrained by pore clogging.

TEM images (Figure 3(a)) of shell-TiO_2 showed that TiO_2 significantly filled pores as nanoparticles with a size less than 50 nm. The X-ray diffraction spectra (Figure 3(b)) of the shell-TiO_2 and neat shell (Figure 3(B1)) suggest that TiO_2 nanoparticles filling shell pores were in several crystal forms. Peaks a1, a2, a3, and a4 in the angle region (2θ values, 25.3, 36.9, 48.0, and 68.8°, resp.) correspond to the XRD standard peaks for anatase (Figure 3(B2)). Peak b in the angle region (2θ values, 44.1°) corresponds to the XRD standard of rutile (Figure 3(B3)). Peaks c1, c2, and c3 in the angle region (2θ values, 30.8, 32.8, and 52.0°, resp.) correspond to the XRD standard of brookite (Figure 3(B4)). The other peaks, unsigned in the curve (Figure 3(b)), also correspond to the amorphous forms for TiO_2 according to standard cards. Based on the results of TEM and XRD, it seems that the TiO_2 loaded within the shell pores are mainly in polycrystalline-like nanostructures.

3.2. Formaldehyde Removal Results. Formaldehyde removal percentage during the 10 hr experiment is shown in Figure 4. The formaldehyde removal percentages at the end of the experiments (10 hr) under both conditions (under continuous illumination at 25°C and under darkness at 25°C) were (70.5 ± 1.2)% and (55.4 ± 1.4)%, respectively. It was obvious that FREI (formaldehyde removal experiments that were carried out under continuous illumination at 25°C) was more efficient than the FRED (formaldehyde removal experiments that were carried out under darkness at 25°C). The formaldehyde removal percentage of FREI was rising continuously during all stages of the experiment, and the formaldehyde removal percentage of FRED was almost constant from 4 hr to 10 hr, though the formaldehyde removal percentage under both conditions did increase markedly during the first three hours (1–3 hr). It should be noted that the formaldehyde

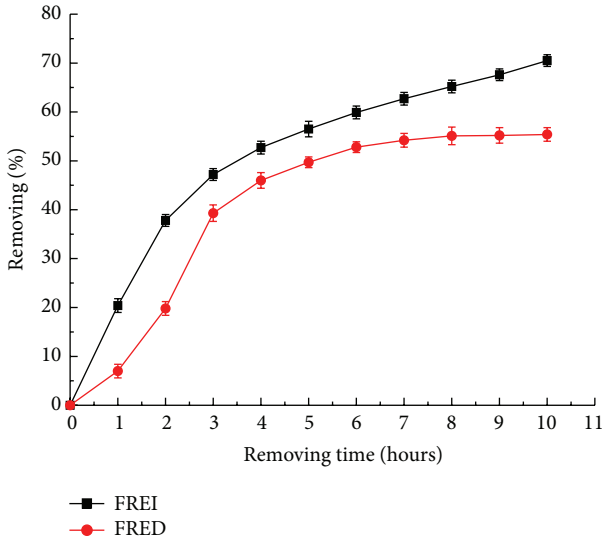

FIGURE 4: Formaldehyde removal percentages. FREI: formaldehyde removal experiments carried out under continuous illumination (about 1500 lx) at 25°C; FRED: formaldehyde removal experiments carried out under darkness at 25°C.

was only adsorbed during the FRED experiments, whereas both adsorption and degradation occurred in the FREI experiments.

It has been known that the superior photocatalytic ability of nano-TiO_2 is due to the decomposition of organic contaminants under the UV light [21, 22]. However, its practical application is limited due to the need for an ultraviolet excitation source (which accounts for only small fraction of solar light) [23]. In order to extend the photoresponse of TiO_2 to the visible region, expand the application of TiO_2, and make an efficient utilization of solar energy, researchers have doped some elements into the nano-TiO_2 matrix. It was proven that Fe-doped nanotitanium dioxide can widen the absorption of the visible light range, enhance the utilization efficiency of visible light, and improve the catalytic performance of nanotitanium dioxide [23, 24]. In the present study, it happens that iron is one of components of *Artemia* egg shells (Figures 2(b), and 2(d)), and the formaldehyde degradation experiment involving shell-TiO_2 composite materials was actualized under visible light. Moreover, the formaldehyde removal percentages in FREI (continuous illumination under visible light) can reach up to (70.5 ± 1.2)%. Therefore, the natural iron in the shells was determined to be connected to the photocatalytic performance of the shell-TiO_2 composite. To prove the function of the natural iron in *Artemia* shells, detailed research will be carried out in future studies.

4. Conclusion

The *Artemia* egg shell with asymptotic reduction pores (diameter: 500 nm–2500 nm) can be used as the carrier for nanocomposite materials. The nanocomposite materials, *Artemia* egg shell-supported TiO_2, were in polycrystalline-like nanostructures and can be used for high efficiency formaldehyde removal (adsorption and degradation) under visible light. Our results would suggest that iron, as one of the shell's natural components, should be associated with the photocatalytic performance of shell-TiO_2 composites. To prove that natural iron in shells broadens the absorption of visible light and enhances photocatalytic efficiency under visible light, detailed research should be carried out in future studies.

Conflict of Interests

The authors declare that there is no conflict of interests regarding the publication of this paper.

Acknowledgments

The authors acknowledge and greatly appreciate the financial support from the National Natural Science Foundation of China (Grant nos. 40830746, 41271102, and 21473153). This work was also financially supported by the Natural Science Foundation of Hebei Province (B2013203108), the Science Foundation for the Excellent Youth Scholars from Universities, the colleges of Hebei Province (YQ2013026), and the Support Program for the Top Young Talents of Hebei Province.

References

[1] X.-P. Liao and B. Shi, "Adsorption of fluoride on zirconium(IV)-impregnated collagen fiber," *Environmental Science & Technology*, vol. 39, no. 12, pp. 4628–4632, 2005.

[2] B. C. Pan, Q. R. Zhang, W. M. Zhang et al., "Highly effective removal of heavy metals by polymer-based zirconium phosphate: a case study of lead ion," *Journal of Colloid and Interface Science*, vol. 310, no. 1, pp. 99–105, 2007.

[3] S. Samatya, Ü. Yüksel, M. Yüksel, and N. Kabay, "Removal of fluoride from water by metal ions (Al^{3+}, La^{3+} and ZrO^{2+}) loaded natural zeolite," *Separation Science and Technology*, vol. 42, no. 9, pp. 2033–2047, 2007.

[4] Q. Zhang, P. Jiang, B. Pan, W. Zhang, and L. Lv, "Impregnating zirconium phosphate onto porous polymers for lead removal from waters: effect of nanosized particles and polymer chemistry," *Industrial & Engineering Chemistry Research*, vol. 48, no. 9, pp. 4495–4499, 2009.

[5] N. Chen, Z. Y. Zhang, C. P. Feng, M. Li, D. Zhu, and N. Sugiura, "Studies on fluoride adsorption of iron-impregnated granular ceramics from aqueous solution," *Materials Chemistry and Physics*, vol. 125, no. 1-2, pp. 293–298, 2011.

[6] H. Tavallali and A. Daneshyar, "Cadmium selenide nanoparticles loaded on activated carbon and its efficient application for removal of fluoride from aqueous solution," *International Journal of ChemTech Research*, vol. 4, no. 3, pp. 1178–1181, 2012.

[7] Q. R. Zhang, B. C. Pan, S. J. Zhang, J. Wang, W. Zhang, and L. Lv, "New insights into nanocomposite adsorbents for water treatment: a case study of polystyrene-supported zirconium phosphate nanoparticles for lead removal," *Journal of Nanoparticle Research*, vol. 13, no. 10, pp. 5355–5364, 2011.

[8] G. van Stappen, "Zoogeography," in *Artemia: Basic and Applied Biology*, T. J. Abatzopoulos, J. A. Beardmore, J. S. Clegg, and

P. Sorgeloos, Eds., pp. 171–224, Kluwer Academic Publishers, Dodrecht, The Netherlands, 2002.

[9] S. Wang and S. Sun, "Comparative observations on the cyst shells of seven *Artemia* strains from China," *Microscopy Research and Technique*, vol. 70, no. 8, pp. 663–670, 2007.

[10] J. E. Morris and B. A. Afzelius, "The structure of the shell and outer membranes in encysted *Artemia salina* embryos during cryptobiosis and development," *Journal of Ultrasructure Research*, vol. 20, no. 3-4, pp. 244–259, 1967.

[11] E. Anderson, J. H. Lochhead, M. S. Lochhead, and E. Huebner, "The origin and structure of the tertiary envelope in thick-shelled eggs of the brine shrimp, *Artemia*," *Journal of Ultrasrucure Research*, vol. 32, no. 5-6, pp. 497–525, 1970.

[12] M. Mazzini, "Scanning electron microscope morphology and amino-acid analysis of the egg-shell of encysted brine shrimp, *Artemia salina* Leach (Crustacea Anostraca)," *Monitore Zoologico Italiano—Italian Journal of Zoology*, vol. 12, no. 4, pp. 243–252, 1978.

[13] K. W. Lee, M. A. Gouthro, D. Belk, and J. R. Rosowski, "Ultrastructure features of the tertiary envelope in the cyst of the brine shrimp *Artemia franciscana* (Anostraca)," in *Proceeding of the 52nd Annual Meeting of the Microscopy Society of America*, G. W. Bailey and A. J. Garratt-Reed, Eds., pp. 362–363, San Francisco Press, San Francisco, Calif, USA, August 1994.

[14] T. Iwasaki, "Tolerance of *Artemia* dry eggs for temperature, vacuum and radiation," *Bulletin de l'Institute International du Froid—Annexe*, vol. 5, pp. 79–88, 1973.

[15] J. S. Clegg, "Desiccation tolerance in encysted embryos of the animal extremophile, *Artemia*," *Integrative and Comparative Biology*, vol. 45, no. 5, pp. 715–724, 2005.

[16] B. J. Finlayson-Pitts and J. N. Pitts, *Chemistry of the Upper and Lower Atmosphere: Theory, Experiments, and Applications*, Academic Press, San Diego, Calif, USA, 2000.

[17] C. M. Schmidt, A. M. Buchbinder, E. Weitz, and F. M. Geiger, "Photochemistry of the indoor air pollutant acetone on Degussa P25 TiO_2 studied by chemical ionization mass spectrometry," *The Journal of Physical Chemistry A*, vol. 111, no. 50, pp. 13023–13031, 2007.

[18] U. Diebold, "The surface science of titanium dioxide," *Surface Science Reports*, vol. 48, no. 5-8, pp. 53–229, 2003.

[19] Z. Ding, H. Y. Zhu, G. Q. Lu, and P. F. Greenfield, "Photocatalytic properties of titania pillared clays by different drying methods," *Journal of Colloid and Interface Science*, vol. 209, no. 1, pp. 193–199, 1999.

[20] A. Rapsomanikis, D. Papoulis, D. Panagiotaras et al., "Nanocrystalline TiO_2 and halloysite clay mineral composite films prepared by sol-gel method: synergistic effect and the case of silver modification to the photocatalytic degradation of basic blue-41 azo dye in water," *Global NEST Journal*, vol. 16, no. 3, pp. 485–498, 2014.

[21] P. Wang, T. Xie, D. Wang, and S. Dong, "Facile synthesis of TiO_2(B) crystallites/nanopores structure: a highly efficient photocatalyst," *Journal of Colloid and Interface Science*, vol. 350, no. 2, pp. 417–420, 2010.

[22] S. Tieng, A. Kanaev, and K. Chhor, "New homogeneously doped Fe(III)-TiO_2 photocatalyst for gaseous pollutant degradation," *Applied Catalysis A: General*, vol. 399, no. 1-2, pp. 191–197, 2011.

[23] Y.-F. Tu, S.-Y. Huang, J.-P. Sang, and X.-W. Zou, "Preparation of Fe-doped TiO_2 nanotube arrays and their photocatalytic activities under visible light," *Materials Research Bulletin*, vol. 45, no. 2, pp. 224–229, 2010.

[24] R. M. Mohamed, D. L. McKinney, and W. M. Sigmund, "Enhanced nanocatalysts," *Materials Science and Engineering R: Reports*, vol. 73, no. 1, pp. 1–13, 2012.